

GONG Observations of Solar Surface Flows

D. H. Hathaway,* P. A. Gilman, J. W. Harvey, F. Hill, R. F. Howard, H. P. Jones, J. C. Kasher, J. W. Leibacher, J. A. Pintar, G. W. Simon

Doppler velocity observations obtained by the Global Oscillation Network Group (GONG) instruments directly measure the nearly steady flows in the solar photosphere. The sun's differential rotation is accurately determined from single observations. The rotation profile with respect to latitude agrees well with previous measures, but it also shows a slight north-south asymmetry. Rotation profiles averaged over 27-day rotations of the sun reveal the torsional oscillation signal—weak, jetlike features, with amplitudes of 5 meters per second, that are associated with the sunspot latitude activity belts. A meridional circulation with a poleward flow of about 20 meters per second is also evident. Several characteristics of the surface flows suggest the presence of large convection cells.

The GONG instruments were designed to measure solar oscillations for helioseismology. The primary data, Doppler velocities, are also an excellent source of information on the nearly steady surface flows. These flows include axisymmetric motions such as differential rotation (in which the equatorial regions rotate more rapidly than the polar regions) and nonaxisymmetric flows such as supergranules (convective flows that tile the sun's surface with thousands of closely packed cells). Although these measurements only characterize the flows in a thin photospheric layer, such information is critical for our understanding of the dynamics of the convection zone and the nature of the magnetic dynamo in this star.

Several components of the surface flows are thought to play leading roles in generating the sun's magnetic field. The differential rotation stretches meridional magnetic field lines to form strong toroidal fields, that is, fields in longitudinal rings about the sun's axis of rotation (1). The meridional circulation transports magnetic flux and angular momentum across parallels of latitude and from one radius to another (2). The nonaxisymmetric convective mo-

tions also redistribute magnetic flux and angular momentum, but in more complex and subtle ways. Here, we report on the first 6 months of GONG measurements of these different flows.

Data Characteristics

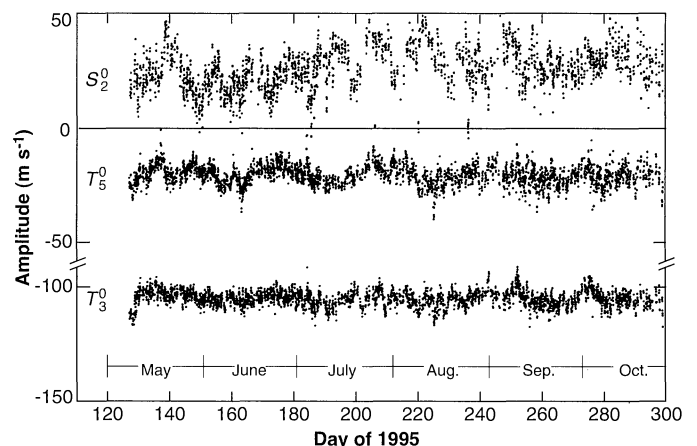
The GONG data have several advantages over most previous data. First, the instruments were specifically designed for accurate Doppler velocity measurements. The Ni I 676.8-nm spectral line was chosen over many other candidate lines because of its isolation from other spectral features, its relative insensitivity to magnetic fields, and its weak dependence on viewing angle from disk center to limb. Second, the instruments were designed to make full disk velocity images at a rapid cadence so that the 5-min p -mode oscillations are well resolved in time. This provides a means for separating this oscillatory signal from the steady flow signal by time averaging. Third, the

supergranulation pattern is resolved by the optics and electronic camera. Fourth, the network of instruments produces nearly continuous coverage, allowing detailed study of the evolution of the convection pattern and of individual cells. Finally, if the network operates for many years, it will be possible to monitor variations in the flow patterns over the course of the solar activity cycle.

The GONG instruments (3) obtain an intensity image, a line-of-sight Doppler velocity image, and a modulation image (which shows variation in the equivalent width of the line) every 60 s. The image geometry is accurately determined, and images are coregistered to within 0.1 pixel and co-aligned to within 0.2° (3, 4). Each image type is averaged over 17 min with a Gaussian-shaped weighting function (5) that reduces the signal attributable to p -mode oscillations with periods shorter than 8 min by a factor of ≥ 100 . These averages are sampled at 4-min intervals. The time-averaged Doppler images are the primary source of information on the surface flows.

These time-averaged Doppler images require special care and handling. The p -mode oscillation signal for helioseismology is obtained by subtracting each Doppler image from the previous one so that the steady signals present in both are removed. With the time-averaged Doppler images, it is the p -mode signals that are largely removed while the steady signals remain. These steady signals include instrumental artifacts along with the desired solar signal. However, because each observation is made by two or more GONG sites in most cases, differencing the observed velocities (after removing the velocity signals produced by Earth's rotation and orbital motion) reveals many of the instrumental signals. Systematic diurnal variations in the measured velocity signals at each site also offer information on instrumental effects. A variety of analysis techniques can be used to extract

Fig. 1. Axisymmetric flow component histories. Hourly measurements of the amplitudes of the dominant meridional flow component (S_2^0) and the two dominant components of the differential rotation (T_3^0 and T_5^0) are plotted as functions of time for the first 6 months of GONG operation. Three instruments produced the earliest measurements, and additional instruments contributed in the later months. All sites show good agreement with each other for both the average values of these component amplitudes and their day-to-day variations.



D. H. Hathaway is in the Solar Physics Branch, Mail Code ES82, Space Sciences Laboratory, NASA/Marshall Space Flight Center, Huntsville, AL 35812, USA. P. A. Gilman is at the High Altitude Observatory, National Center for Atmospheric Research, Post Office Box 3000, Boulder, CO 80303, USA. J. W. Harvey, F. Hill, R. F. Howard, J. W. Leibacher, and J. A. Pintar are at the National Solar Observatory, National Optical Astronomy Observatories (NSO/NOAO), Post Office Box 26732, Tucson, AZ 85726-6732, USA. H. P. Jones is at NASA/Goddard Space Flight Center, Southwest Solar Station, NSO/NOAO, Post Office Box 26732, Tucson, AZ 85726-6732, USA. J. C. Kasher is in the Physics Department, University of Nebraska at Omaha, 64th and Dodge Streets, Omaha, NE 68182-0266, USA. G. W. Simon is at Air Force Materiel Command, Phillips Laboratory, Geophysics Directorate, Solar Research Branch, NSO, Sunspot, NM 88349, USA.

*To whom correspondence should be addressed.

information about the surface flows and their interactions with the magnetic field elements. Most of the results we describe are derived from a technique that fits the data with mathematical functions that represent the various flow components (6, 7). Other results come from techniques that determine the flows by tracking Doppler or magnetic features over time intervals of hours or days (8).

Axisymmetric Flows

The axisymmetric flows are the differential rotation and meridional circulation. The fluid velocities associated with these flows are given by expansions in terms of spherical harmonic functions with

$$v_{\theta}(\theta) = - \sum_{\ell=1}^N S_{\ell}^0 P_{\ell}^1(\cos \theta) \quad (1)$$

$$v_{\phi}(\theta) = \sum_{\ell=1}^N T_{\ell}^0 P_{\ell}^1(\cos \theta) \quad (2)$$

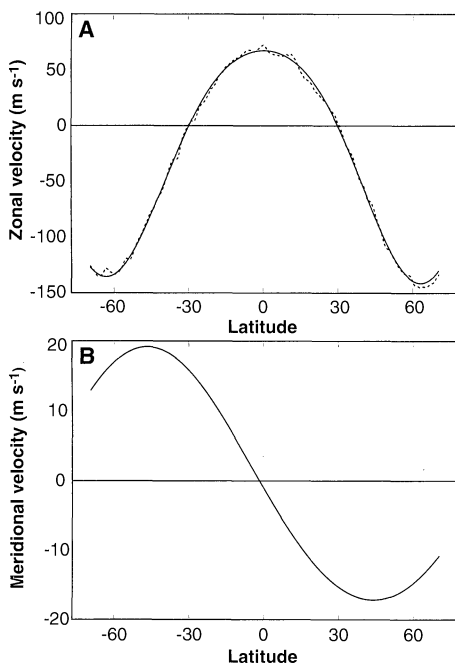


Fig. 2. (A) Differential rotation profile for May 1995. The differential rotation profile as a function of latitude is plotted as a dotted line; positive velocities are in the direction of the basic rotation. The spherical harmonic fit to this profile is shown as a solid line. This profile gives more rapid rotation at the equator and a slight north-south asymmetry. (B) Meridional circulation profile for May 1995. The spherical harmonic fit for the meridional circulation is plotted as a solid line. No data points are plotted here because the meridional flow is determined by fitting a two-dimensional velocity pattern to the data rather than by extracting a signal at each latitude. This profile gives poleward flow from the equator in two cells (positive velocities point southward).

where v_{θ} is meridional velocity, v_{ϕ} is rotation velocity, θ is colatitude (heliocentric angle from the north pole), ϕ is longitude, P_{ℓ}^1 are associated Legendre polynomials of degree ℓ and order 1 (9), and S_{ℓ}^0 and T_{ℓ}^0 are coefficients that characterize the velocity components. In practice, the sums in Eqs. 1 and 2 are terminated at $N = 8$, but only four terms dominate the flow (Fig. 1). The largest of these, $T_1^0 = 2043 \text{ m s}^{-1}$, represents the solid-body rotation of the sun. The second and third terms, T_3^0 and T_5^0 , characterize the differential rotation, and the fourth term, S_2^0 , describes the meridional circulation. Over the first 6 months of operation, these terms give

$$v_{\theta}(\theta) = -54 \cos \theta \sin \theta \text{ m s}^{-1} \quad (3)$$

$$v_{\phi}(\theta) = (1837 - 195 \cos^2 \theta - 342 \cos^4 \theta) \sin \theta \text{ m s}^{-1} \quad (4)$$

with statistical errors of $\sim 1 \text{ m s}^{-1}$ for each coefficient. These results are in fair agreement with results from many earlier studies (10, 11). The exception is the weaker solid-body rotation component, which is also smaller than that given by the helioseismic measurements (12).

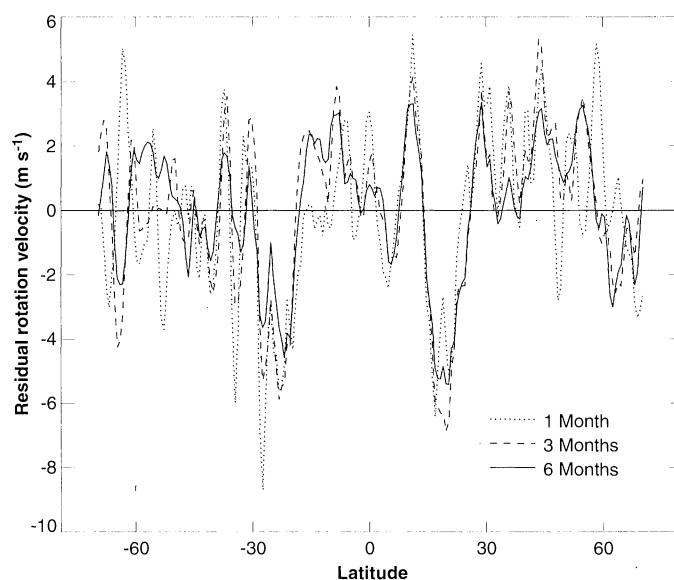
The meridional flow has been notoriously difficult to measure. Both the amplitude and the direction of this flow have been in question because of large uncertainties in the measurements. The primary difficulty is in separating the meridional flow signal from the convective blue shift, a velocity signal produced by the correlation between outward velocities and brightness in the small, unresolved granules. Specialized techniques (6, 7) are required to separate the meridional flow from the other solar signals. Although the daily scatter for S_2^0 is somewhat larger than that for T_3^0 and T_5^0 , short-term variations are evident because

the uncertainty is so much smaller than that seen in earlier studies. Areas of the surface that are populated by strong magnetic fields are masked out in the analysis (6, 7), so day-to-day and week-to-week variations in these coefficients may be caused by signal leakage from nonaxisymmetric flow patterns.

The differential rotation profile (Fig. 2A) is dominated by two components that give a rapidly rotating equator and a slowly rotating pole. The meridional flow profile (Fig. 2B) is dominated by one component that gives a net flow away from the equator and toward the poles. There is no sign of the equatorward flows near the equator and poles reported in pattern tracking studies (13). All components up to and including $\ell = 8$ are included in these profiles, but the other components contribute only a few meters per second on average, and the day-to-day variations in their measured amplitudes are of similar size. Of these smaller components, the T_2^0 component represents an asymmetry in the rotation rate of the two hemispheres. Its average value over this 6-month period was $-7.8 \pm 0.3 \text{ m s}^{-1}$, which indicates that the southern hemisphere was rotating slightly more rapidly than the northern hemisphere. Observations made with the GONG prototype instrument before the deployment of the network showed a stronger asymmetry in the summer of 1994. Two higher degree components of the meridional circulation, S_4^0 and S_6^0 , also have small but significant amplitudes ($-1.6 \pm 0.5 \text{ m s}^{-1}$ and $-1.3 \pm 0.1 \text{ m s}^{-1}$, respectively), and earlier measurements indicate changes in these components as well.

We extracted the rotation profile (Fig. 2A) from a fit to the rotation signal at each latitude. This signal is given by the gradient

Fig. 3. Residual rotation signal averaged over three intervals. The difference between the measured rotation signal and the spherical harmonic fit to that signal is plotted as a function of latitude. The jetlike torsional oscillation signal is identified with the fairly broad ($\sim 15^\circ$ wide) dips that are seen in all three averages. The latitudes of these features (18°N and 22°S) are slightly poleward of the latitudes where sunspots were found during this period. The narrower features are attributed to signal leakage from the nonaxisymmetric cellular flows.



in the Doppler velocity measured east-to-west along a solar latitude. Earlier studies (11, 14) have shown that there are additional velocity features in the rotation signal. These features, called torsional oscillations, consist of jetlike disturbances that first appear at high latitudes and move toward the equator during each solar cycle. These features have amplitudes of $\sim 5 \text{ m s}^{-1}$ and latitudinal widths of 10° to 15° . During the May–October 1995 time interval, the velocity minima were reported to be located at 18°N and 22°S (15). Despite its feeble nature, this signal was already apparent from only 1 month of GONG data (Fig. 3).

Cellular Flows

Cellular convective flows also play important roles in the dynamics of the sun's convection zone and the generation of the sun's magnetic field. Supergranule flows concentrate magnetic flux along the borders of the cells where these cellular flows converge. These magnetic flux concentrations are the source of chromospheric emissions that dominate the structure of the sun's upper atmosphere. Giant cells several times as large as typical supergranules are thought to be responsible for maintaining the sun's differential rotation and meridional flow (2, 16). Searches for giant cells over the last 30 years have been inconclusive (17). Because theoretical arguments for their existence are contradictory (18), observations are needed to settle the issue. The cellular flows can be studied by projecting the Doppler velocity signal onto the nonaxisymmetric spherical harmonic functions. The resulting spectrum (Fig. 4) has a prominent peak at spherical harmonic degree $\ell \sim 80$, which gives cells with diameters of $\sim 50,000 \text{ km}$ —somewhat larger than the $30,000 \text{ km}$ typically measured for supergranules.

The spectrum extends to larger and

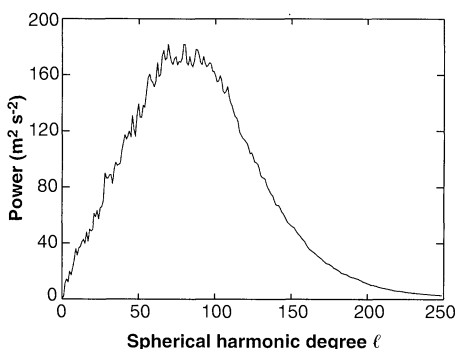


Fig. 4. Cellular flow spectrum. The sum of the squared amplitudes at each spherical harmonic degree ℓ is plotted for May 1995. This spectrum has not been corrected for attenuation resulting from image blurring at large values of ℓ . Correction of this attenuation will increase the power substantially above $\ell \sim 100$.

smaller cell sizes. With the present instrumental configuration, GONG measurements are limited by spatial resolution to degrees less than ~ 250 . Degrees of 500 or more are needed to represent the smaller cells identified as mesogranules (19), and degrees of more than 4000 are needed to represent granules. Giant cells would have degrees smaller than ~ 30 , so the low end of the spectrum is particularly interesting. The total power for degrees less than 10 gives a velocity signal with an amplitude of less than $\sim 10 \text{ m s}^{-1}$. Portions of this signal may be the source of the week-to-week variations seen in the axisymmetric flow amplitudes (Fig. 1).

Tracking Horizontal Flows

Feature tracking (8) provides another method for measuring the surface flows. The time-averaged Doppler images contain features whose motion can be followed to give the velocity vector along the solar surface. In this respect, these measurements complement the Doppler signal to give vector velocity information. First, the axisymmetric flows are removed from the data. The remaining signal consists of the cellular flow patterns; these images are projected onto maps in heliographic longitude and latitude. Data strips in longitude at each observed latitude are correlated with similar strips taken hours or days later. A maximum in the correlation between the two strips occurs when they are shifted to account for the sun's rotation. The size of the shift divided by the time difference gives the rotation rate of the pattern; the strength of the correlation indicates how much the pattern has evolved. This process is taken one step further by filtering the cellular velocity signal so that it only contains cells with a limited range of sizes. The velocity spec-

trum (Fig. 4) is subdivided into five spectral bands: $1 \leq \ell < 16$, $16 \leq \ell < 32$, $32 \leq \ell < 64$, $64 \leq \ell < 128$, and $128 \leq \ell$. Typical supergranules are represented by the fourth and fifth of these bands, whereas giant cells are represented by the first two bands.

Results from this analysis (Fig. 5) show that the cells in all five spectral bands rotate with the sun. Slight differences are found for the rotation rates of the various cell sizes, but these differences do not appear to be significant given the variations found in the measurements. The synodic rotation rate of the photosphere, averaged over latitudes within 30° of the equator, is $\sim 13.2^\circ \text{ day}^{-1}$. The rotation rate for the cellular features in these five spectral bands is somewhat faster at $\sim 13.7^\circ \text{ day}^{-1}$.

Discussion

Some of our results are at odds with those of previous studies. The rotation rate is $\sim 10\%$ weaker than that found earlier (10, 11) and is similarly discrepant with the helioseismic results (12). The rotation signal is represented by the average gradient in the Doppler velocity across the sun. Instrumental signals with similar properties are found in the GONG data. Although differences between instruments can be corrected by means of simultaneous observations, any gradients common to all instruments cannot be determined this way. Other sources of this weaker signal include the effect of scattered light and difficulties in determining the absolute velocity scale. The meridional flow is about twice as strong as that found using magnetic features (13) and does not show any evidence of equatorward flow; this may be an indication of a variation in meridional flow speed as a function of depth. The GONG measurements represent the fluid motions in the photosphere,

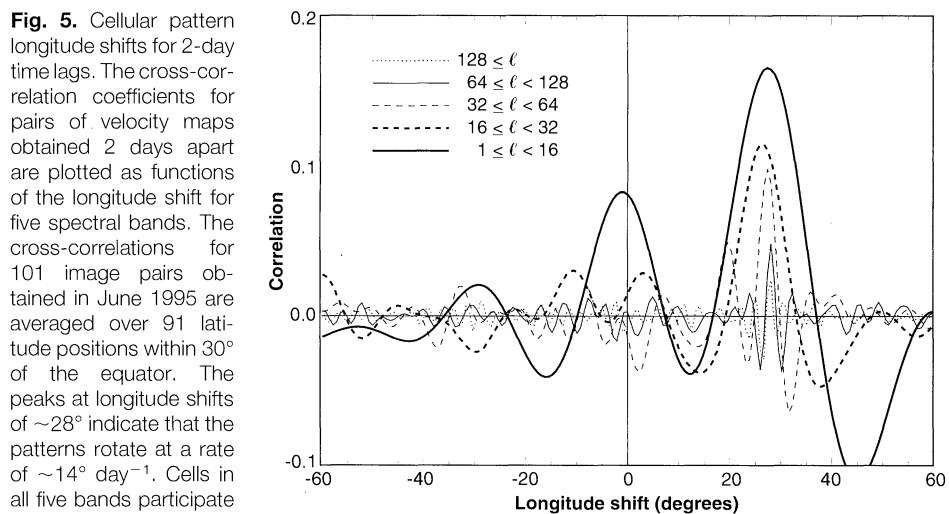


Fig. 5. Cellular pattern longitude shifts for 2-day time lags. The cross-correlation coefficients for pairs of velocity maps obtained 2 days apart are plotted as functions of the longitude shift for five spectral bands. The cross-correlations for 101 image pairs obtained in June 1995 are averaged over 91 latitude positions within 30° of the equator. The peaks at longitude shifts of $\sim 28^\circ$ indicate that the patterns rotate at a rate of $\sim 14^\circ \text{ day}^{-1}$. Cells in all five bands participate in the sun's rotation. The stronger correlations for the larger cells indicate that they live longer than the smaller cells.

whereas the motions of magnetic features represent some average over the depths to which these features extend. Numerical simulations of the effects of solar rotation on the convective motions in these outermost layers indicate that the poleward meridional flow should decrease with depth (20). Another possibility is that the meridional flow speed may also vary in time.

The appearance of the torsional oscillation signal is somewhat surprising. Previous observing programs used years of data to extract these features. Although the residual rotation signal from a single month (Fig. 4) is rather noisy, the broad, deep dips are quite evident and were identified with the torsional oscillation signal before any efforts were made to identify their positions from other sources. Also surprising are the many narrow features that appeared to persist for the entire 6 months. These axisymmetric flow components should be dynamically linked. The Coriolis force on a poleward meridional flow opposes the observed differential rotation, whereas the same force acting on the differential rotation would tend to reverse the meridional flow (2, 16). We might expect that any variations seen in one component might be reflected in others as we monitor these flows over the solar cycle.

Several observations suggest that giant-cell convection patterns may be extracted from these data. The convection spectrum exhibits power at all degrees down to $\ell = 1$. Variations seen in the measured rotation and meridional circulation components are consistent with the presence of large-scale nonaxisymmetric flow patterns. Another

indication of the presence of giant cells is the finding that the largest cellular patterns have components that rotate at a rate commensurate with the sun's rotation rate.

Improvements to the GONG instruments are planned. Higher magnification will allow us to study a broader range of cell sizes and may provide details that enhance the results from feature tracking. Another promise of the GONG network is that we will obtain these data for many years. The variations of the flow patterns over the course of the next solar cycle will provide us with answers as well as more questions concerning the dynamics of this star's convection zone and the nature of its activity cycle.

REFERENCES AND NOTES

1. W. M. Elsässer, *Phys. Rev.* **69**, 202 (1946); H. W. Babcock, *Astrophys. J.* **133**, 572 (1961); E. N. Parker, *Cosmical Magnetic Fields* (Clarendon, Oxford, 1979); P. R. Wilson, *Solar and Stellar Activity Cycles* (Cambridge Univ. Press, Cambridge, 1994).
 2. P. A. Gilman, *Geophys. Astrophys. Fluid Dyn.* **8**, 93 (1977); _____ and J. Miller, *Astrophys. J. Suppl. Ser.* **61**, 585 (1986).
 3. J. W. Harvey *et al.*, *Science* **272**, 1284 (1996).
 4. F. Hill *et al.*, *ibid.*, p. 1292.
 5. The weighting function for the time average is derived from K. Libbrecht and H. Zirin, *Astrophys. J.* **308**, 413 (1986) with weights
- $$W(\delta t) = \exp\left(-\frac{\delta t^2}{2\tau^2}\right) - \exp\left(-\frac{\Delta t^2}{2\tau^2}\right) \left[1 + \left(\frac{\Delta t^2}{2\tau^2}\right) - \left(\frac{\delta t^2}{2\tau^2}\right) \right] \quad (5)$$
- where δt is the time difference from the central observing time, $\tau = 4$ min is the half-width of the filter, and $\Delta t = 9$ min is the half-length of the filter.
6. D. H. Hathaway, *Sol. Phys.* **108**, 1 (1987); *ibid.* **137**, 15 (1992).
 7. _____, *Astrophys. J.* **460**, 1027 (1996).
 8. T. L. Duvall, *Sol. Phys.* **63**, 3 (1979); H. B. Snodgrass and R. K. Ulrich, *Astrophys. J.* **351**, 309 (1990); R. W. Komm, R. F. Howard, J. W. Harvey, *Sol. Phys.* **145**, 1 (1993); H. P. Jones, in *Fourth SOHO Workshop Helioseismology*, T. Hoeksema, V. Domingo, B. Fleck, B. Battrick, Eds. (ESA SP-376, ESA, Noordwijk, Netherlands, 1995), vol. 2, pp. 227-232; L. H. Strous, *ibid.*, pp. 213-217 and 219-222.
 9. The specific normalization of the associated Legendre polynomials is described in (7).
 10. P. H. Scherrer, J. W. Wilcox, L. Svalgaard, *Astrophys. J.* **241**, 811 (1980).
 11. R. K. Ulrich *et al.*, *Sol. Phys.* **117**, 291 (1988).
 12. M. J. Thompson *et al.*, *Science* **272**, 1300 (1996).
 13. H. B. Snodgrass and S. B. Dalley, *Sol. Phys.* **163**, 21 (1996); S. Latushko, *ibid.*, p. 241.
 14. R. F. Howard and B. J. LaBonte, *Astrophys. J.* **239**, L33 (1980); H. B. Snodgrass, *ibid.* **291**, 339 (1985).
 15. The dips in the torsional oscillation signal seen at Mount Wilson observatory occurred at 18°N and 22°S during May-October 1995 (R. Ulrich, personal communication).
 16. G. A. Glatzmaier and P. A. Gilman, *Astrophys. J. Suppl. Ser.* **45**, 351 (1981).
 17. R. Howard, *Astrophys. J.* **228**, L45 (1979); B. J. LaBonte, R. Howard, P. A. Gilman, *ibid.* **250**, 796 (1981); J. Kuhn, *ibid.* **264**, 689 (1983); H. B. Snodgrass and R. Howard, *ibid.* **284**, 848 (1984); J. M. Robillot, R. Bocchia, E. Fossat, G. Grec, *Astron. Astrophys.* **137**, 43 (1984); B. R. Durney, L. E. Cram, D. B. Guenther, S. L. Keil, D. M. Lytle, *Astrophys. J.* **292**, 752 (1985).
 18. G. W. Simon and N. O. Weiss, *Z. Astrophys.* **69**, 435 (1968); H. Yoshimura, *Astrophys. J. Suppl. Ser.* **52**, 363 (1983); G. W. Simon and N. Weiss, *Mon. Not. R. Astron. Soc.* **252**, 1 (1991).
 19. L. J. November, J. Toomre, K. B. Gebbie, G. W. Simon, *Astrophys. J.* **245**, L123 (1981).
 20. D. H. Hathaway, *Sol. Phys.* **77**, 341 (1982).
 21. GONG is managed by NSO, a division of NOAO that is operated by the Association of Universities for Research in Astronomy under cooperative agreement with NSF. The data were acquired by instruments operated by the Big Bear Solar Observatory, High Altitude Observatory, Learmonth Solar Observatory, Udaipur Solar Observatory, Instituto de Astrofísica de Canarias, and Cerro Tololo Inter-American Observatory.

18 March 1996; accepted 9 May 1996